Failure Investigation of Rear Axle Taper Roller Bearing by Using the Vibration Spectrum

Junaid Ali · Deepak Borse ⓘ

Abstract Prevention of the occurrence of field failures of taper roller bearings under high-load and moderate-speed application is the prime challenge for bearing manufacturers. Failures result from numerous defects in bearing, such as localized or distributed defects. Various controls have been aligned in the manufacturing process to prevent outflow of defective bearings to end-application. However, still a part in million skips the controls in process and gets assembled in final application. In this literature, experiments are conducted to study the effect of grinding defect on cone track surface of taper roller bearing using the vibration spectrum, due to its peculiar unidentifiable nature in regular manufacturing process. Vibration analysis techniques are discussed in this case study. Statistical and spectrum analysis results are shared and concluded at the end of this case study.

Keywords Rolling element bearing · Failure analysis · Vibration · Manufacturing defects

List of Symbols
Z Number of rollers
D_{RO} Roller diameter
D_P Pitch circle diameter
α Contact angle

Abbreviations
BPFI   Ball pass frequency of inner race
BPFO   Ball pass frequency of outer race
BSF   Ball spin frequency

J. Ali · D. Borse (✉)
National Engineering Industries Ltd, Jaipur, Rajasthan, India
e-mail: deepak.borse@nbcbearings.in

J. Ali
e-mail: junaid.ali@nbcbearigs.in

FTF   Fundamental train frequency
RPM   Rotation per minute of shaft

Introduction

Historically, various researchers have made the contribution in vibration analysis of rolling element bearings using numerous methodologies such as time-domain and frequency-domain analysis techniques to identify incipient defects on the surface of rolling element bearing. Before the occurrence of failure, there are various methodologies available for fault diagnosis of rolling element bearing, such as time-domain analysis, frequency-domain analysis, time–frequency-domain analysis and many others [1].

Time-domain analysis is basically a statistical analysis of parameters, i.e., RMS, crest factor (ratio of peak and RMS of acceleration), kurtosis of the time-domain waveform. As per ISO 15242, Part 1 crest factor of a waveform should be less than 3. If the crest factor is more than 3, then it suggests that the signal consists of a number of peaks. A lower value of the crest factor represents good health of bearing. However, in this study, we have demonstrated that with the increase in the severity of incipient defects on the bearing surface, the value of crest factor becomes equal to that of good bearing because with the increase in defect severity the RMS value decreases which randomizes the overall crest factor. Similarly, as per ISO 15242, for Part 1 the value of kurtosis should be less than 3 for good bearing and if the value is higher than 3, then it suggests that some defect must be present in the bearing. Likewise, with the increase in the severity of defect the value of kurtosis randomizes and becomes approximately equivalent to that of good bearing. Moreover, kurtosis and crest factor only

tell us about the presence of a defect in a bearing. It does not give any idea about the location of the defect on bearing components. Frequency-domain vibration analysis technique converts time-domain waveform into frequency-domain waveform using fast Fourier transform or FFT. Fast Fourier transform is the upgraded version of discrete Fourier transform having swift signal processing. All rotating components of machinery have rolling element bearings to reduce friction and support load. Under application of high load and high RPM, the defect on the bearing surface comes under load zone, which gives rise to an impulse. Those impulses repeat it, periodically giving rise to pulses of vibration at a particular frequency which is known as "Characteristic Frequency of Defect." Every time, the defect comes into contact with the mating surface; under the load zone, a sharp peak can be observed in frequency waveform against the corresponding defect frequency which is also known as ball pass frequency. The main advantage of using a frequency-domain approach over time-domain approach is that it provides the location of the defect in the bearing. Whenever a fault occurs in any of the bearing components, peaks generate at the frequency corresponding to defect frequency where the amplitude of peak depends on the severity of defect in bearing [2–6].

Some of expressions for bearing characteristic frequencies are shown below:

In frequency-domain vibration analysis technique, the frequency envelope or waveform is a graphical illustration of acceleration vs. frequency (50–10 K Hz). The vertical axis represents the displacement, velocity or acceleration, whereas the horizontal axis represents the time or frequency of vibration. The entire bandwidth of 50–10 K Hz is divided into three bands, i.e., low band, medium band and high band [7]. Possible causes for the generation of peaks in lower band are misalignment of spindle or shaft, looseness of component and stiffness differential of clamps. In middle band, peaks are generated due to either surface waviness or chatter on raceway. Two-point or three-point roundness of raceway surface creates disturbances in the middle band of frequency spectra. If there are incipient defects present in the bearing, then every time the defect passes from the load zone; it will give rise to a pulse of vibration at the corresponding defect frequency of component which repeats harmonically at $1\times$, $2\times$, $3\times$ and so on [8].

Experimental Details

Single-side vibration testing machine is used in this study. It is constructed for testing taper roller bearings vibration with high rotating speed. It is equipped with spindle, motor transmission measuring unit sending pressurization,

loading path and hydraulic system to provide preload to taper roller bearing, a piezoelectric vibration sensor to detect mechanical vibrations and an acoustic sensor. Machine specifications are shown in Appendix—Table 3. The reference photograph of actual test setup is shown in Fig. 1.

Test bearing mounted over spindle and initial load was applied through hydraulic cylinder arrangement for better vibration spectrum results. First, good bearing was mounted over the setup to gather baseline data for further comparative analysis. Then, bearing with defect on cone track raceway was mounted for testing. Accelerometer sensor was mounted over cup OD surface perpendicular to the axis of rotation of spindle. Acoustic sensor was mounted in the vicinity of bearing to capture and record audible noise in frequency range.

Contact-type piezoelectric accelerometer sensor is mounted 90° to outer diameter of outer ring. Sensor positioning is the most important part of setup installation. Improper sensor mounting may give abrupt results. As per ISO 15242, Part 1, accelerometer sensor should be mounted perpendicular to the axis of rotation of bearing to get reliable results. NBC-made tapered roller bearing 32010 is used in the study. Bearing specifications are listed in Table 1.
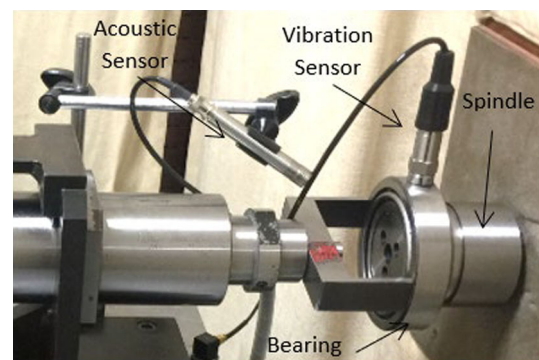

Fig. 1 Vibration analysis experiment test setup

Table 1 NBC 32010 bearing specifications

S. No.	Parameters	Specification
1	Outer diameter	90.00 mm
2	Inner diameter	50.00 mm
3	Total width	21.75 mm
4	Roller diameter	10.859 mm
5	Roller length	14.961 mm
6	Number of rollers	19
7	Contact angle	31° 17′ 04″
8	Pitch circle diameter	70.00 mm

J Fail. Anal. and Preven. (2020) 20:1091–1096

1093

Defect Description

A good bearing was used to collect baseline data for comparative study, and a defective bearing was produced for experimentation. Defect was generated on cone track surface using surface grinder to produce a similar to regular production grinding job-stop damage as shown in Fig. 2. The experimentation was performed particularly for the job-stop type of defect and it is due to the peculiarity and unidentifiable nature in the regular manufacturing process. Such defects depreciate bearing's service life and produce noise and vibration in application it is fitted.

Defect Dimensions

Assume a defect as a perfect rectangle vertically along the length of the mating surface of outer and inner rollers, respectively. Defect dimensions are shared in Table 2. Cone track surface roundness profile was measured on Talyrond. Roundness traces are shown in Fig. 3. Measurement scale was 5 μm/Div with Gaussian filter type and filter range of 1–150 μm.

Defect Surface Profile

Defect surface profile was traced on 3D and 2D profilometers. Defect has approximately 9 μm depth and 2.9 mm width. Surface profile traces are shown in Figs. 4 and 5.
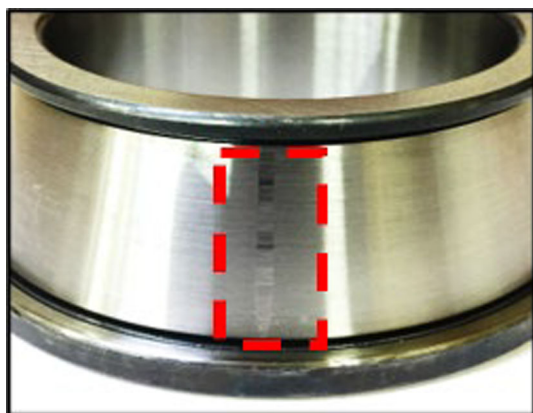

Fig. 2 Damage cone track surface of taper roller bearing

Table 2 Cone track surface defect dimensions

Parameter	Length (mm)	Width (mm)	Depth (mm)	Area (mm^2)
Cone track surface	22.450	1.4	0.0125	31.43

Results

To collect baseline data, a good 32010 bearing mounted over testing equipment and required initial loading was applied. Few drops of lubrication oil was added to prevent bearing from burning while running at a high rotational speed of 0–5000 rpm. The average test time was 5 s. Vibration analysis waveform was plotted on the Hann window as shown in Figs. 6, 7 and 8 using MATLAB software.

Vibration analyzer data are analyzed on MATLAB software, and several graphs are plotted for good and defective bearings. As shown in Fig. 6, the FFT spectrum does not have peaks in the lower band region of frequency band, whereas in defective bearing spectrum a significant rise in peaks can be seen having maximum acceleration peak value of approx. 0.05 m/s^2. As shown in Fig. 7, in the middle-band spectrum of good bearing a distortion is visible; however, maximum amplitude of 0.025 m/s^2 of spectrum is significantly low to contribute to the overall vibration of bearing, whereas in defective bearing maximum amplitude of spectrum is as high as 0.09 m/s^2 which will contribute to the overall vibration of bearing. Moreover, there is a continuous rise in amplitude over 900 Hz, which dimmed drastically in a higher band of the spectrum as shown in Fig. 8. The amplitude of vibration has shown appreciable declination and some peaks appear negligibly low amplitude. Contrary to good spectrum in higher band of defective bearing spectrum, it is visible that amplitude values are high and the maximum amplitude value is approx. 0.26 m/s^2 at 4000 Hz. Overall, amplitude of
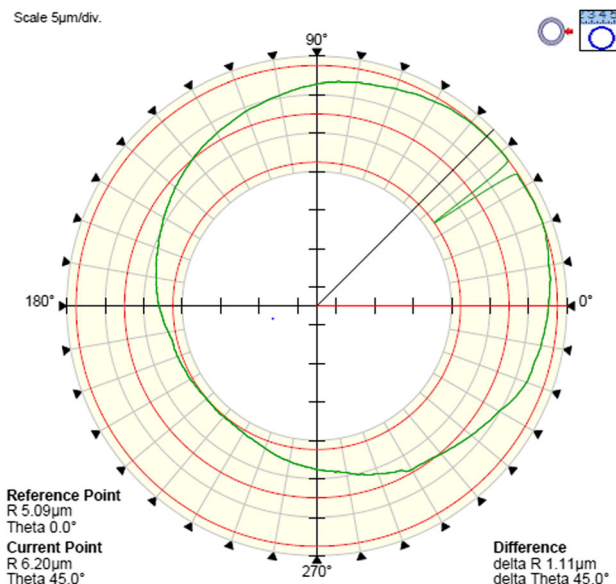

Fig. 3 Defect roundness profile using Talyrond^{TM} roundness measurement machine

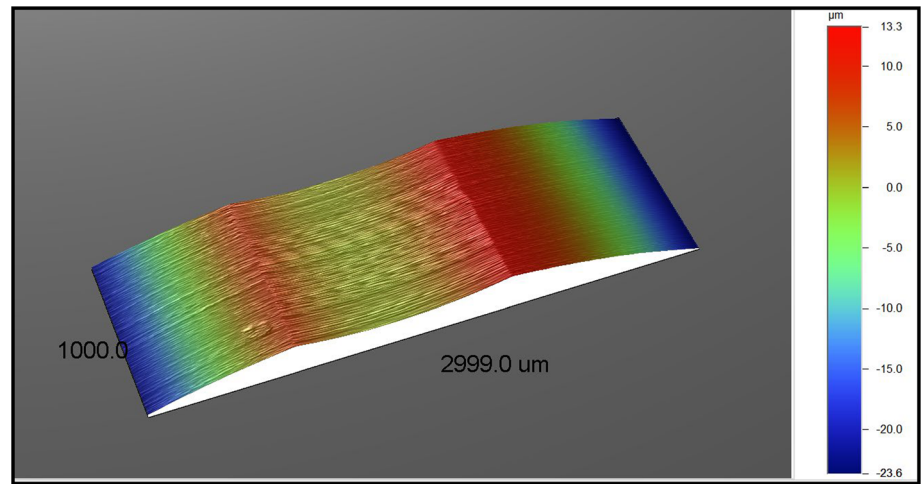**Fig. 4** 3D surface profile of defect on cone track surface

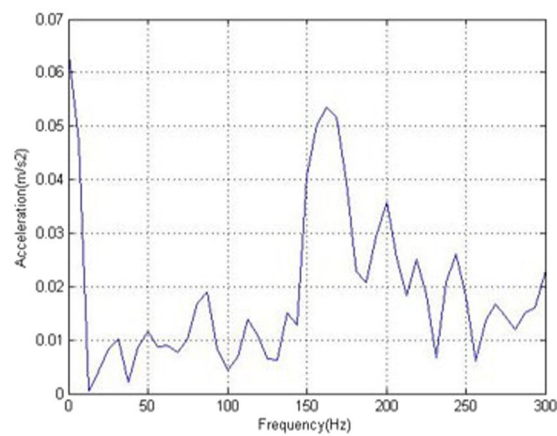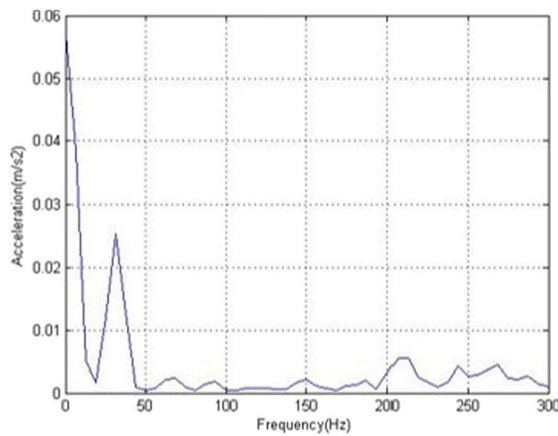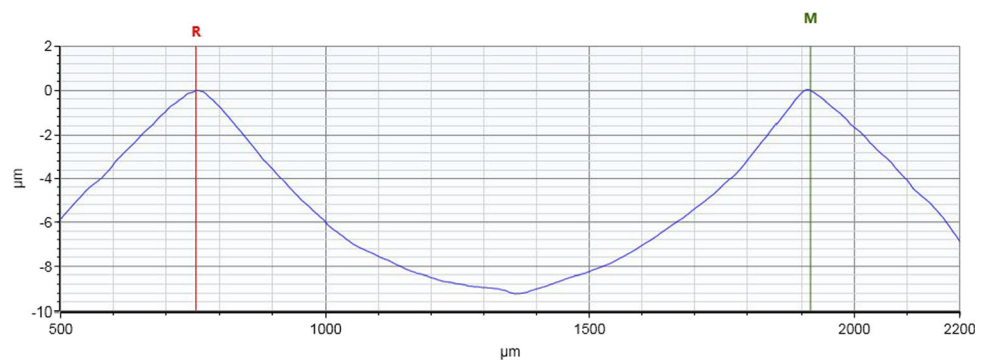**Fig. 5** 3D surface profile of defect on cone track surface

Fig. 6 Good vs. defective bearing—L BAND

defective bearing has risen significantly from lower band to higher band in contrast to good bearing which is a desired result for the case study. In higher band, a maximum peak of the spectrum, i.e., 0.26 m/s^2, was achieved at 4000 Hz in defective bearing, whereas a peak amplitude of approx. 0.025 m/s^2 in the middle band was achieved for good bearing.

Conclusion

The study reveals the effect of good bearing and defective bearing used in axle application. The premature failures occur due to lack of quality inspection methods. The authors have demonstrated the lesson learned from the quality techniques. It is essential to monitor the methods and understand the application scenario for high-load and
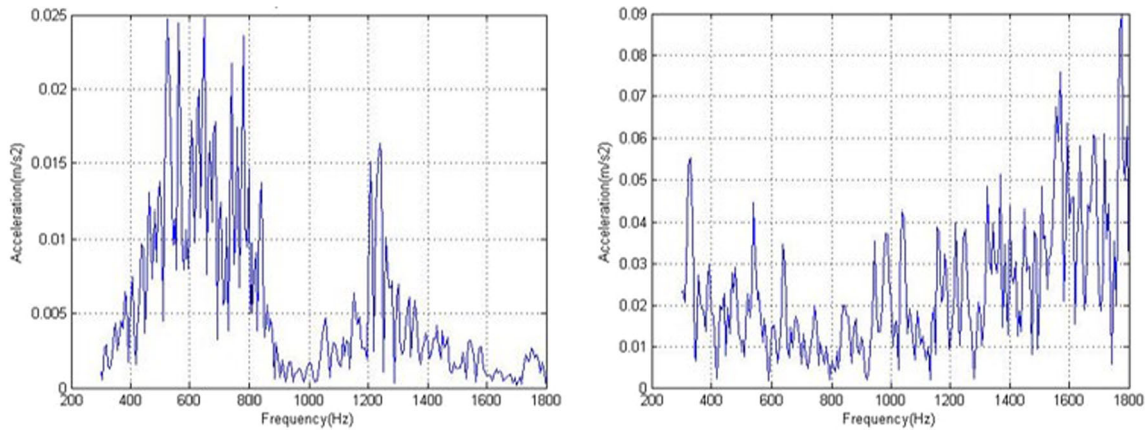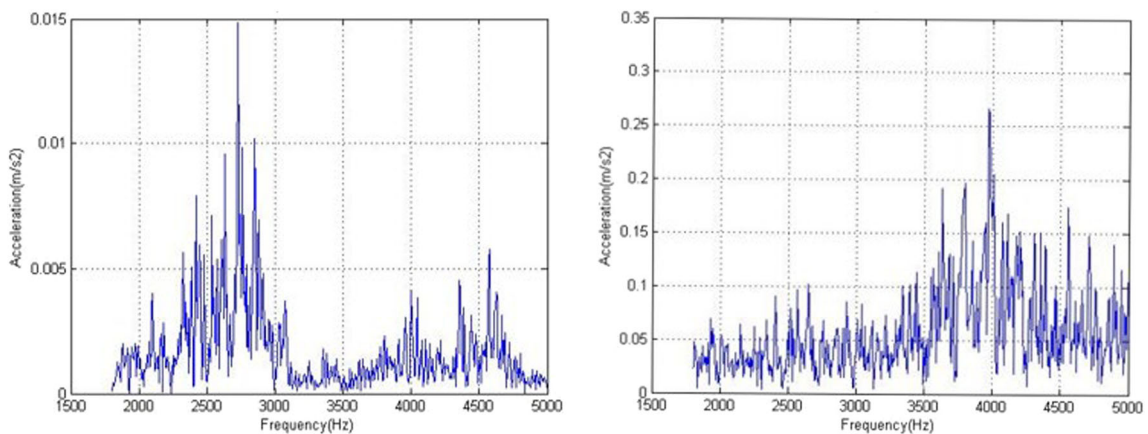
Fig. 7 Good vs. defective bearing—M BAND

Fig. 8 Good vs. defective bearing—H BAND

moderate-condition axle bearing. Vibration analysis, especially by spectrum technique, is the adequate way to capture the failure occurred in bearing.

Appendix

$$\text{BPFI} = \frac{Z}{2}\left[1 + \left(\frac{D_{RO}}{D_p}\right)\cos\alpha\right] * \frac{\text{RPM}}{60} \quad \text{(Eq 1)}$$

$$\text{BPFO} = \frac{Z}{2}\left[1 - \left(\frac{D_{RO}}{D_p}\right)\cos\alpha\right] * \frac{\text{RPM}}{60} \quad \text{(Eq 2)}$$

$$\text{BSF} = \left(\frac{D_{RO}}{2D_p}\right)\left[1 + \left(\frac{D_{RO}}{D_p}\right)2\cos 2\alpha\right] * \frac{\text{RPM}}{60} \quad \text{(Eq 3)}$$

Table 3 Machine specifications

S. No.	Parameter	Specification
1	Bandwidth	L: 50–300 Hz
		M: 300–1800 HZ
		H: 1800–5000 Hz
2	Sensitivity	100 mg/V
3	Axial load	1T max.
4	Power	1.0 kW
5	Speed	50–5000 r.p.m.

$$\text{FTF} = 1/2\left[1 - \left(\frac{D_{RO}}{D_p}\right)\cos\alpha\right] * \frac{\text{RPM}}{60} \quad \text{(Eq 4)}$$

See Table 3.

1096

J Fail. Anal. and Preven. (2020) 20:1091–1096

References

1. S. Patidar, P.K. Soni, An overview on vibration analysis techniques for the diagnosis of rolling element bearing faults. IJETT **4**(5), 1804–1809 (2013)

2. N. Tandon, B.C. Nakra, Vibration and acoustic monitoring techniques for the detection of defects in rolling element bearings—a review. Shock Vibr. Digest **24**(3), 3–11 (1992)

3. N. Tandon, A. Choudhury, A review of vibration and acoustic measurement methods for the detection of defects in rolling element bearings. Tribol. Int. **32**, 469–480 (1999)

4. A.K. Gupta, V.K. Sharma, Failure of ball bearings and its diagnosis by vibration analysis. Chem. Eng. World **24**(5), 45–49 (1989)

5. J. Mathew, R.J. Alfredson, The condition monitoring of rolling element bearings using vibration analysis. Trans. ASME J. Vibr. Acoustics **106**, 447–453 (1984)

6. N. Tandon, G.S. Yadava, K.M. Ramakrishna, A comparison of some condition monitoring techniques for the detection of defect in induction motor ball bearings. Mech. Syst. Signal Process **21**, 244–256 (2007)

7. N. Tandon, B.C. Nakra, Detection of defects in rolling element bearings by vibration monitoring. J. Inst. Eng. (India) **73**, 271–282 (1993)

8. J. Mais, *Spectrum Analysis—the key features of analyzing spectra,* SKF USA Inc., CM5118 EN, May 2002

Publisher's Note Springer Nature remains neutral with regard to jurisdictional claims in published maps and institutional affiliations.